communications earth & environment

ARTICLE

https://doi.org/10.1038/s43247-023-00883-6 OPEN

Neoproterozoic reorganization of the Circum-Mozambique orogens and growth of megacontinent Gondwana

Chao Wang [1]✉, Xian-qing Jing[2]✉ & Joseph G. Meert[3]

The serpentine orogenic belts that formed during the Neoproterozoic assembly of Gondwana resulted in geodynamic changes on the planet in advance of the Cambrian radiation. The details of Gondwana assembly associated with the closure of the Mozambique Ocean are enigmatic. We compile published geological and paleomagnetic data to argue that the Tarim block was associated with the Azania and Afif–Abas–Lhasa terranes and they were the locus of long-lived Andean-type subduction during the ~900–650 Ma interval. Our model suggests a subduction system reorganization between 750-720 Ma, which resulted in two distinct phases of Mozambique ocean evolution. Between 870-750 Ma, a N-S oriented subduction system marks the locus of ocean crust consumption driven by the extension of the Mozambique Ocean. Beginning ~720 Ma, a newly developed ~E-W oriented subduction system began to consume the Mozambique Ocean and led to the assembly of eastern Gondwana. Our new reconstruction uses true polar wander to constrain the relative paleo-longitude of Tarim, South China and West Africa. In this scenario, the closure of the Mozambique Ocean and formation of Gondwana was orthogonal to the preceding supercontinent Rodinia.

[1] State Key Laboratory of Continental Dynamics, Department of Geology, Northwest University, 710069 Xi'an, China. [2] College of Resources, Environment and Tourism, Capital Normal University, 100048 Beijing, China. [3] Department of Earth & Planetary Sciences, University of Florida, Gainesville, FL 32611, USA. ✉email: chaowang@nwu.edu.cn; jingxq@cnu.edu.cn

The growth of megacontinent Gondwana resulted from plate reorganization following the breakup of Rodinia during the late Neoproterozoic–Cambrian interval. Gondwana assembly involved the suturing of different blocks within the East African, Brasiliano, Damara and Kuunga orogens and concomitant destruction of the Mozambique, Brasiliano, and Damaran oceans[1–8]. The East African Orogen (EAO) is a long-lived (>400 Ma) accretionary-style margin at one side of the Mesoproterozoic–Neoproterozoic Mozambique Ocean, which separated India and Azania (central Madagascar, Somalia, eastern Ethiopia and Arabia) from the rest of Africa[6–9]. Azania collided with eastern parts of Africa between 640 and 600 Ma[6]. This was followed by final Gondwana amalgamation between 550 and 500 Ma[1–3]. The assembly of Gondwana coincides with a period of Earth's history marked by dramatic changes in atmospheric circulation, oceanic circulation, the rapid motion of continents, nucleation of the inner core, hyperactive reversing magnetic field, a decrease of geothermal gradients along subduction zones, climatic variations, steep increase in O_2 and the rise of metazoan life[10–17].

From a geodynamic perspective, the closure of the Mozambique Ocean along the EAO can be examined in the context of supercontinent assembly and breakup via introversion, extroversion, or orthoversion[18,19], which is related to the evolution of the structure of the lower mantle structure beneath Africa[20,21]. Despite the numerous controversies and general lack of high-quality palaeomagnetic data during the Late Ediacaran, the paleogeographic evolution leading to the closure of the Mozambique Ocean and the development of the EAO is vital for constraining the evolution of the Neoproterozoic Earth system.

Various models that deal with the progressive assembly of Gondwana have been proposed[2–6,22,23]. Recently, coeval Neoproterozoic orogenic activity was identified in the Tarim craton[24] and the Lhasa Terrane hinting at possible links to orogenic events in eastern Gondwana[25]. In this paper, we compile available geological, geochronological, and paleomagnetic data to present a new orthoversion model for the breakup of Rodinia, closure of the Mozambique Ocean, and amalgamation of central Gondwana.

The Mozambique Ocean and the East African Orogen

The Mozambique Ocean was one of three prominent ocean basins that existed or formed during the Rodinia breakup[1,6,7,26,27]. The Mozambique Ocean closed as India and Azania converged with eastern Africa (Kalahari, Congo, Sahara metacraton) during the East African Orogeny[1–3]. The EAO encompasses most of eastern Africa extending from the Arabian-Nubian Shield (ANS, in the north) to Mozambique (in the south). Sandwiched within the EAO lies a broad band of Archean to Paleoproterozoic crust between the Indian Shield and Congo–Tanzanian Cratons that were identified Azania and the Afif–Abas terranes[28] (Fig. 1). The Azania block and the Afif–Abas terrane (the Al-Mafid Terrane in Yemen and Abas terrane into Saudi Arabia) were isolated microcontinents within the Mozambique Ocean[28]. Geochronologic and structural evidence suggests that Azania separated as a ribbon continent from the Congo–Tanzania Craton[29,30]. The Mozambique Ocean was subdivided into a West and East branch by Azania at ~750 Ma[6,31]. Closure of the Mozambique Ocean involved island-arc collisions and microcontinent accretion (ca. 1080–650 Ma) followed by continental collision with the Congo craton and Saharan Metacraton between ca. 650 and 620 Ma along the length of the EAO (for review see Fritz et al.[32]). Younger orogenic events in eastern Gondwana include the ~550–520 Malagasy Orogeny between Azanian-Afif-Abas and western India[3] and coeval Kuunga Orogeny which completed the amalgamation of eastern Gondwana[2].

Based on the published geological and geochronologic results (Fig. 2, Supplementary Data), each of these sub-regions within the EAO is described below.

The Arabian–Nubian Shield. Meso- to Neoproterozoic age island arcs, including volcanic rocks, gneisses, and sedimentary protoliths, are recognized in the ANS and developed between ca. 1.03–0.93 Ga and ca. 0.87–0.73 Ma[31–36]. In addition, numerous dismembered fore-arc and back-arc ophiolites are found throughout the ANS[37–39]. Blueschist-facies metamorphic assemblages have been reported from slices within western portions of the ANS[40]. Subduction, volcanic arc formation, and terrane accretion (ca. 830–650 Ma) overlap with migmatization and high-grade metamorphism (T: 700–850 °C and P: 0.7–0.9 GPa) (dated at ~775 Ma and 720–715–Ma[34, 41,42]). The granitoids in the ANS show early arc-related affinities followed by collision-related calc-alkaline assemblages (~715–700 Ma), subsequent calc-alkaline post-collisional (~640–600 Ma), anorogenic alkaline A-type granitoids and volcanics (~620–550 Ma), and finally by post-collisional extension as exemplified by the intrusion of mafic–felsic dikes (591–545 Ma)[42–44]. Although local variations exist, an age of ~620 Ma is proposed for the cessation of subduction and initiation of the post-collisional extensional regime in the western ANS[34,35,44,45].

Neoproterozoic basement of Oman. Basement rock exposure is limited in Oman, which is currently located on the eastern side of the ANS. The volcanic and intrusive activity extended from 850 to 785 Ma and was followed by the emplacement of granodiorite around 750 Ma and culminated with the intrusion of mafic dyke swarms at ~620 Ma[46–48]. Collision-related metamorphic and intrusive activity ceased around 750 Ma resulting in a relatively strong lithosphere and establishing a fundamental tectonic boundary in the central part of the Arabian plate dividing it into two distinct domains[6,49] (Fig. 1). Because of the differences in the tectonic history, geochemistry, and geology, Oman is proposed to have occupied a position closer to NW India and Pakistan during the mid-late Tonian[49].

The Mozambique belt. The Neoproterozoic MB represents the central and southern regions of the EAO and consists of high-grade granulite- and amphibolite-facies rocks[2,50,51]. Most published zircon U–Pb age data on metamorphic zircons, metamorphic rims on igneous zircons are well grouped between ~650 and 620 Ma[52,53]. At least two collisional events occurred within the MB, the first between ~650 and ~620 Ma, particularly in the eastern and western granulite belts, and the second at ~550 Ma, especially along the more southern reaches of the MB including the Tanzania Craton and farther east in Madagascar where it has reached regional ultrahigh-temperature metamorphism (UHTM) conditions[2,53–55] (Fig. 2).

Madagascar. Madagascar is made up of several domains with Archean to Neoproterozoic rocks. Intrusive igneous rocks formed between 1080 and 900 Ma are restricted to the Ikalamavony domain in southern Madagascar, which was interpreted to represent a magmatic arc and marginal volcano-sedimentary sequence within a continental back-arc tectonic setting outboard of the Antananarivo domain[56–61]. 850–750 Ma granitoids and gabbros are widespread throughout Madagascar[57,58,61]. Younger, 750–720 Ma volcanic, granitoid, and sedimentary rocks are developed in the Bemarivo domain of northern Madagascar[59,62]. There are ~670–630 Ma intermediate-felsic volcanic and intrusive rocks developed in the Vohibory and Androyan–Anosyan domains of South Madagascar[63,64]. Central and South

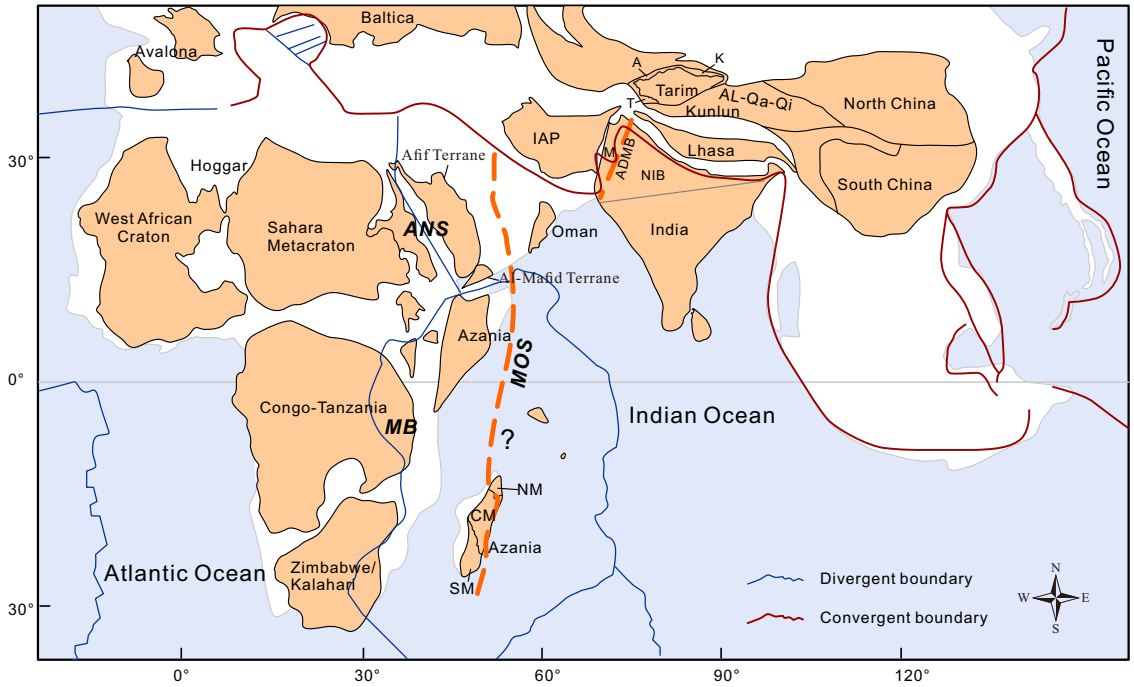

Fig. 1 Distribution of Africa and Eurasian continental crust, ocean basins and plate boundaries at 0 Ma (modified after Merdith et al.[7]). Light brown polygons are areas of continental lithosphere in the Neoproterozoic that our model used, White polygons are areas of present-day continental lithosphere. ANS Arabian–Nubian Shield; Al Altyn Tagh, Qa Qaidam, Qi Qilian, MB Mozambique belt, NM Northern Madagascar, CM Central Madagascar, SM Southern Madagascar, IAP Iran–Afghanistan–Pakistan, ADMB Aravalli–Delhi mobile belt, M Mewar block, NIB North Indian Block, T Tiekelike, A Aksu, K Kuluketage, MOS Inferred final Mozambique Ocean Suture (after Collins et al.[6]).

Madagascar were deformed and underwent amphibolite to granulite facies metamorphism between ~650 and 610 Ma[57,63–65] (Fig. 2). Ediacaran–Early Cambrian (580–510 Ma) post-collisional granitic magmatism, regional metamorphism, and deformation occurred throughout Madagascar (Fig. 2). This younger magmatism overlaps with the latter stages of high-grade metamorphism in northern Madagascar between ca. 550 and 530 Ma (750–850 °C and 6–8 kbar)[64,65]. In central Madagascar, U-Pb metamorphic ages obtained from zircon rims range from 670 to 540 Ma[57]. In southern Madagascar, high-temperature and ultra-high temperature (UHTM) metamorphism took place between 580 and 510 Ma based on ages from metamorphic monazite in metapelite, and igneous zircons, and monazite in syn- and post-tectonic granitoids[57,63–67] (Fig. 2). The tectonic history of Madagascar is controversial. Collins and Windley[28] divide Madagascar along the Betsimaraka suture and include the central and northern regions into Azania. According to the Azania model, central/northern Madagascar collided with the Dharwar craton sometime prior to the final amalgamation of Gondwana. Another model, the so-called SMIWH (South Madagascar–India–Wanni-Highland) model, posits a Paleoproterozoic assembly of these regions around 1.8 Ga from then until the breakup of Gondwana[68]. More recently, central and southern Madagascar were separated into two distinct domains[64]. The Vohibory–Graphite–Androyen domains represent the 'western' region of Madagascar on one side of the Mozambique Ocean whereas the Anoysen-Ikalamavony domains were positioned on the other side. In that model, the final Madagascar assembly took place at ca. 580–520 Ma, and the Beraketa high-strain zone marks the closure of the Mozambique Ocean.

The Tarim Craton. The Tarim Craton is made up of Archean to Neoproterozoic rocks covered by younger desert deposits that hinder direct outcrop sampling. There are two main areas (Tiekelike and Altyn Tagh–Dunhuang) at the southern margin of the Tarim basin, and the Aksu and Kuluketage areas at the northern margin of the Tarim basin (Fig. 1). In previous models, the Central-South Altyn was considered an integral part of the Tarim Craton; however, the Central-South Altyn is now thought to represent an exotic terrane accreted after the late Neoproterozoic[69]. The northern margin (N Tarim) is characterized by late Mesoproterozoic–Neoproterozoic tectonothermal events at (Fig. 2; see Ge et al.[24] for a review): (1) ca. 1050–900 Ma granitic magmatism and arc volcanic rocks; (2) ca. 830–750 Ma K-rich adakitic granite, 823–800 Ma mafic dykes, 816–787 Ma high-pressure granulites and ca. 830 Ma crustal anatexis; (3) ca. 780–700 Ma basic dykes, volcanic rocks, and granites, ca. 750–730 Ma Aksu blueschists; (4) 680–600 Ma basic dykes, basalt, leucogranites and alkaline/ferroan/A-type granites. These data suggest that N Tarim represents a long-term subduction-accretion arc built along the northern Tarim margin between ca. 1050 and 600 Ma. These ages correspond well with tectonic events in the East African Orogen (Fig. 2). In the Tiekelike and West Kunlun regions along the southwestern margin of the Tarim Craton (SW Tarim), there are ca. 900–880 Ma within-plate bimodal volcanic rocks[69], OIB-type basic dykes which formed at 802 ± 9 Ma and the Kudi bimodal igneous complex which crystallized at 783 ± 10 Ma[70]. Between ca. 0.9–0.7 Ga, SW Tarim evolved as a passive margin with alluvial and shallow-marine deposition and within-plate bimodal volcanism[69].

The Lhasa Terrane. The Lhasa terrane (southern Tibetan Plateau) is located between the Qiangtang and Tethyan Himalayan terranes (Fig. 1). The Lhasa terrane contains a suite of Neoproterozoic meta-sedimentary rocks, meta-diabase/gabbro, and meta-granite, which have undergone amphibolite–HP granulite-facies metamorphism and varying degrees of deformation[25]. Recent studies indicate that the Lhasa terrane is characterized by ca. 930–902 Ma rift-related magmatic and sedimentary rocks[71,72],

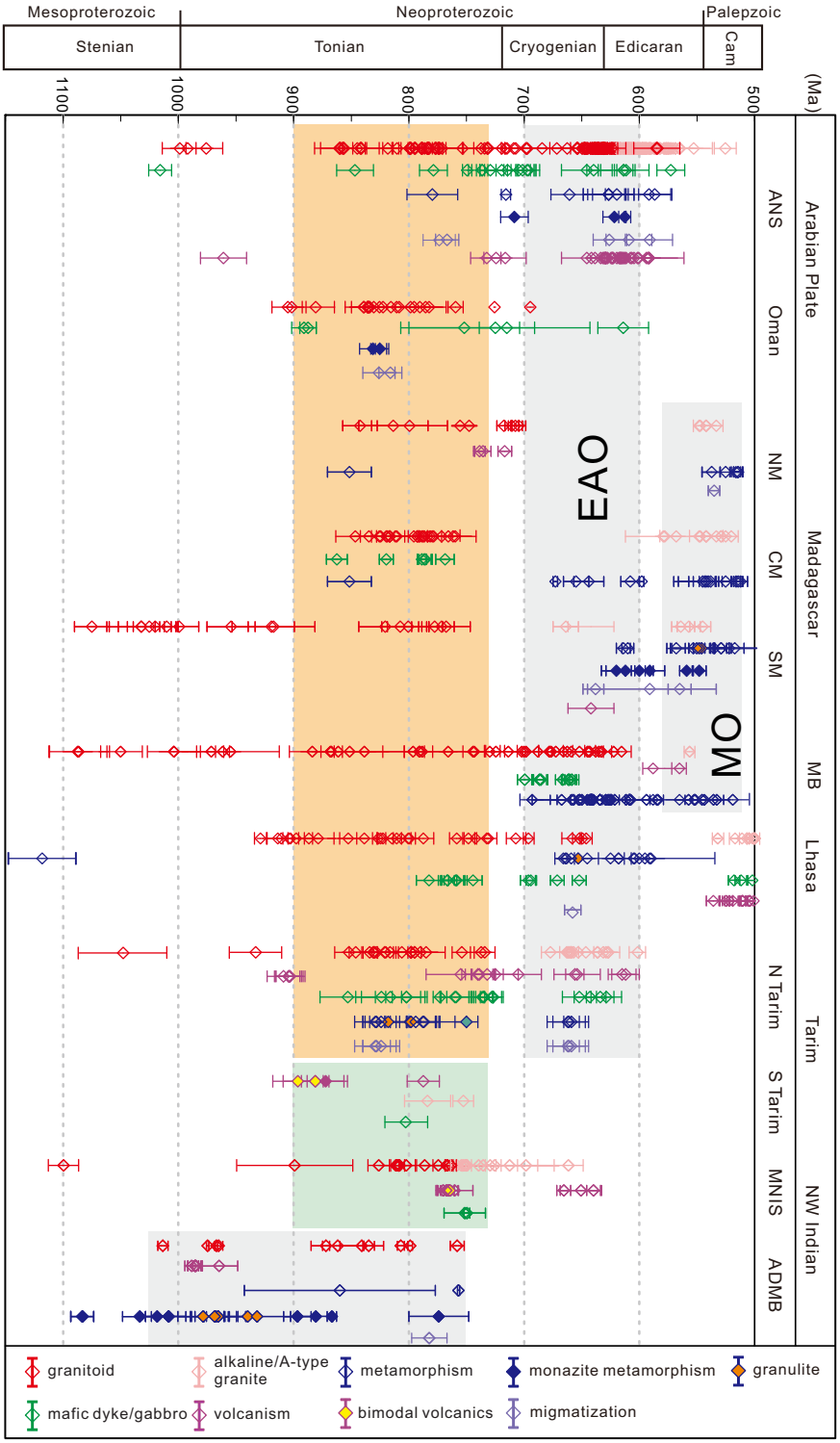

Fig. 2 Late Meoproterozoic-Cambrian magmatic or metamorphic events. Error bars represent the 1-sigma uncertainties. Data source in Supplementary Data. Cam Cambrian, ANS Arabian–Nubian Shield, MB Mozambique belt, NM Northern Madagascar, CM central Madagascar, SM Southern Madagascar, MNIS Malani–Nagar igneous rocks, ADMB Aravalli–Delhi mobile belt. EAO East African Orogen; MO Malagasy Orogen. See text for details, sources, and discussion. Orange, gray, and green shadings are accretion, collision, and rifting/extensional settings, respectively.

ca. 830–700 Ma arc-related calc-alkaline and tholeiitic mafic rocks and granitoids (Fig. 2); followed by ca. 690–650 Ma collision-related magmatism and HP granulite-facies peak-metamorphism metamorphism and amphibolite-facies metamorphism at 605–590 and 480 Ma[25,73]. ~530–470 Ma high-K calc-alkaline and shoshonitic granitoid emplacement along with ~530–495 Ma A-type ultrapotassic rhyolites indicate a post-collision setting or an extensional environment associated with an active margin[74].

NW India. The 1.1–0.8 Ga Aravalli–Delhi mobile belt (ADMB) of NW India marks a Late Mesoproterozoic–Neoproterozoic

subduction–collision orogen, thought to be associated with the collision of the Marwar Block with the North Indian Block during Rodinia assembly[75,76] (Fig. 1). The ca. 1.1–0.9 Ga metamorphic event is widespread in metapelites, ortho- and paragneisses, which are characterized by a metamorphic transition from *HP* granulite to *HP* amphibolite facies along clockwise P–T paths[77]. Widespread Meso–Neoproterozoic aged volcano-plutonic rocks constitute major parts of the southern segment of the Delhi Fold Belt (SDFB). Peak metamorphic conditions in the SDFB were followed by isothermal decompression[78]. The intrusion of the 'Erinpura granites' is coeval with the timing of shear activity and retrograde metamorphism of granulite exhumation in the DFB (830–820 Ma)[79,80]. The youngest Neoproterozoic igneous activity in the region (770–700 Ma) constitutes the Malani Igneous Province[81] (NW India) and coeval plutonic rocks in the Nagar Parkar region[82] (Pakistan) where ages overlap with Malani but also evidence for magmatic activity as young as ~650 Ma. The Marwar block is extensively intruded by the Erinpura and related granites, and in several places has been covered by younger volcano-sedimentary sequences belonging to the Sindreth, Punagarh, and Marwar groups. The Malani igneous rocks include voluminous felsic lavas and tuffs (occasionally bimodal at the base), granite emplacement, and felsic and mafic dyke intrusions[75,81]. Because felsic volcano-plutonic rocks are distributed over a large area >100,000 km^2 in NW India, SE Pakistan, Seychelles, and Mauritia this late-Neoproterozoic magmatic episode has been regarded as a silicic LIP[83]. Some have argued that the Malani–Nagar–Parkar LIP formed in an extensional setting[81–83]. The debate regarding the tectonic setting for Malani magmatism is far from settled as support for an active Andean-type margin has been argued based on similar-aged magmatic activity in Seychelles, Madagascar, and Mauritia[80,84–87].

Results and discussion

Ca. 900 Ma Southern Tarim connection with Congo, West Africa, and Lhasa in the southern hemisphere. Traditionally, Tarim is positioned either between Australia and Laurentia[88,89] or close to north India or west Australia in Rodinia[90,91]. However, these locations are difficult to reconcile with the contrasting tectonic settings in north and south Tarim. Geologic evidence from northern Tarim indicates an active continental margin[24] and supports a peripheral location of Tarim in Rodinia. However, the development of a rift margin in southwestern Tarim around 900 Ma[92], contradicts both the "missing-link"[89] and peripheral reconstruction models of Tarim in Rodinia. In those reconstructions, Tarim is placed in the northern hemisphere[88–91]. The northern hemispheric choice is presumably based on Tarim's early Paleozoic affinity with eastern Gondwana. Despite this common assumption, there is no a priori reason to rule out a southern hemisphere position for Tarim between 900 and 800 Ma as discussed below (Supplementary Table 1, Fig. 3). Here we compile high-quality Neoproterzoic paleomagnetic poles from Tarim (Supplementary Table 1, reliability score (R) ≥ 5[93]), and find that a southern hemisphere placement of Tarim before the Ediacaran is possible. We demonstrate that by reversing the 900–720 Ma palaeopoles from Tarim (all poles are listed in Supplementary Table 1), we can generate a simpler APWP through the Neoproterozoic (Fig. 3a). By inverting these poles, we reduce the arc distance between 720 and 635 Ma poles dramatically (from 129.7° to 50.3°) and decrease the APW rates from 17 to 6.5 cm yr^{-1}, We, therefore, propose a palaeomagnetically based reconstruction with Tarim located in southern hemisphere until the Ediacaran (Figs. 3b and 4). Geological evidences are also offered to support our conjecture.

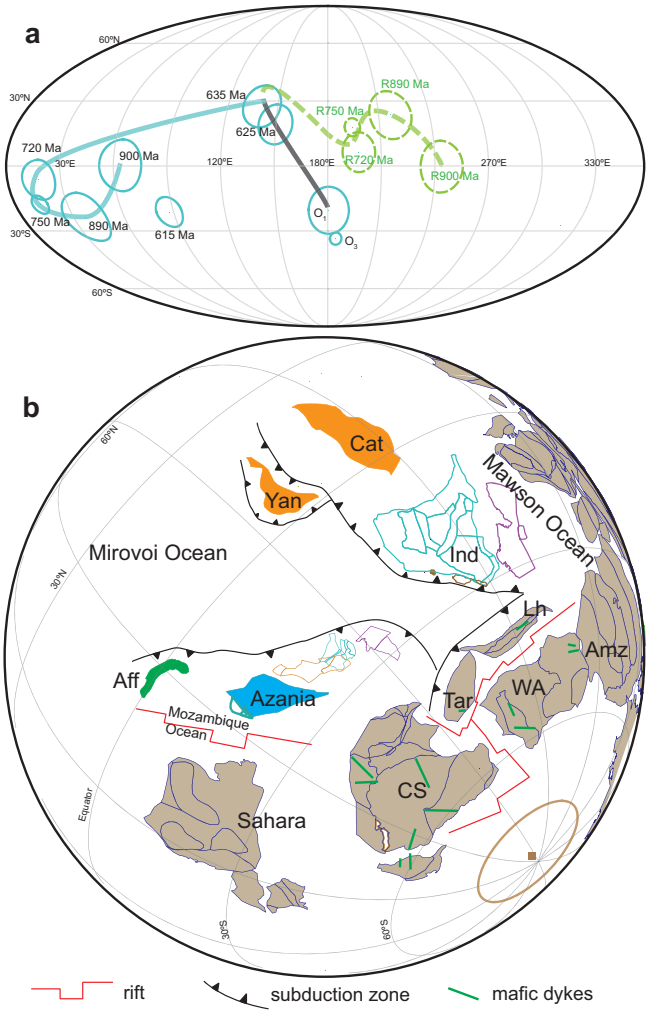

Fig. 3 New Rodinia reconstruction based on paleomagnetic and geological data. a Neoproterozoic paleomagnetic poles of Tarim, all are listed in Supplementary Table 1. Blue colors are traditionally interpreted as north poles used to place Tarim in the northern hemisphere[7]; green colors with dashed circles are reversed poles, assuming that Tarim was located in the southern hemisphere. O_1 and O_3 are early and late Ordovician poles from Tarim. **b** Reconstruction of Rodinia at 900 Ma. Brown-shadowed continents are parts of Rodinia. CS, Congo-São Francisco, Tar Tarim, WA West Africa, Lh Lhasa, Amz Amazonia, Ind India, Yan Yangtze, Cat Cathysia. Brown square with a circle is the 900 Ma pole of Tarim. Euler rotation parameters for India, Yangtze, Lhasa, Tarim, and Congo-São Francisco are listed in Supplementary Table 2, others are after Merdith et al.[7].

It is generally accepted that Congo-São Francisco, West Africa, and the Lhasa block were assembled in the southern hemisphere during the Neoproterozoic era[71]. Several rift-related provinces developed during the 900-880 Ma interval on many of these blocks indicating large-scale breakup. In SW Tarim, ca. 900-870 Ma bimodal volcanic and ca. 900–850 Ma A-type granites were used to argue for an intraplate rift setting[91, 92,94]. The Bahia–Gangila large igneous province (LIP) in Congo-São Francisco suggests two stages of (950–910 and 890–870 Ma) lithospheric stretching and rifting[95]. Previous studies based on these ca. 900 Ma rift-related LIPs, and Mesoproterozoic magmatism hint at a possible link between South Tarim, North China, and Congo–São Francisco[92]. Although all of these continents record 900–860 Ma magmatism, Tarim has no record of rift-related magmatism between 950 and 910 Ma in contrast to

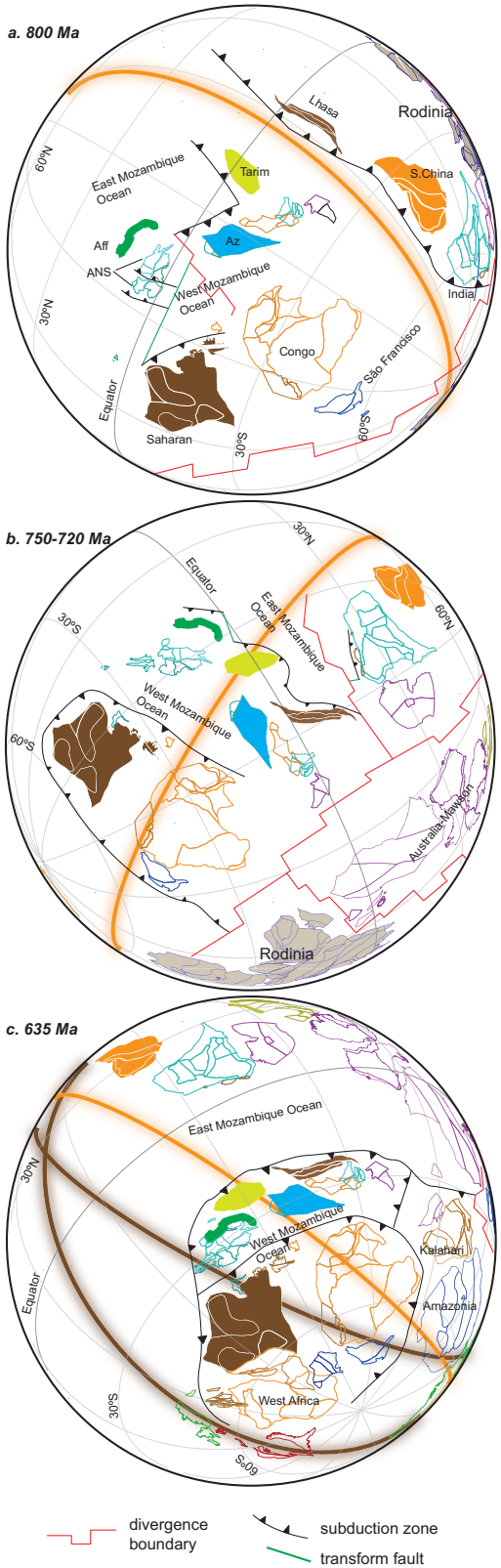

Fig. 4 Paleogeographic reconstruction focused on breakup of Rodinia and evolution of Mozambique Ocean and Gondwana. a 800 Ma, **b** 750 Ma, **c** 635 Ma. Aff Afif-Abas, Az Azania, ANS Arabian-Nubian Shield, S. China South China. Orange and brown curves are fixed true polar wander trajectories (great-circles) between 810–790 and 615–570 Ma for South China (orange) and West Africa (brown).

prominent magmatism in both Congo-São Francisco and North China. Therefore, we question the proposed links between Tarim and North China or São Francisco. However, on the (present-day) eastern side of Congo, bimodal volcanic and sedimentary rocks in the Zambezi and Lufilian belts in Zambia and the Sankuru-Mbuji-Mayi-Lomami-Lovoy failed-rift basin indicate rifting in southeast Congo between ~890 and 800 Ma[96]. This history is broadly similar to events in SW Tarim. We propose a link between SW Tarim and the Congo Zambezi belt during the 1.0–0.9 Ga interval. Dyke swarms in the Anti-Atlas region of West Africa (Iguerda-Taïfast LIP, ~885-860 Ma), Hoggar and Reguibat shield (~850–800 Ma) are consistent with a rift setting in West Africa[97]. Mafic dyke swarms also are reported from Ghana at 915 and 860 Ma[98]. Geochronological studies on mafic rocks in northern Lhasa indicate a late-stage rift setting at ca. 900 Ma[71]. We place the Lhasa terrane close to Ghana and near southern India between 1000 and 900 Ma. The mafic rift volcanism may represent a LIP beneath eastern Congo, west Africa, Lhasa, and Tarim. Our placement of Lhasa, India, South China, and Tarim (LIST) in the southern hemisphere at 900 Ma changes the size of the Mozambique Ocean and creates a separate Mawson Ocean between LIST and Australia-East Antarctica (Fig. 3b). We also position subduction zones adjacent to Azania and along the western margin of India which are not present in other full-plate models at 900 Ma (see Fig. 15 in Merdith et al.[7]).

Neoproterozoic long-lived Andean-type subduction zone and terranes in the EAO. Northern Tarim is characterized by Andean-style subduction-accretion from 900 to 650 Ma which closely parallels the tectonic environment in the ANS, MB, central and southern Madagascar, but is strikingly different from northern Australia and western Laurentia in this period[99].

If our ca. 900 Ma southern hemisphere paleogeographic reconstruction for LIST is correct (Fig. 3), then there is a marginal subduction setting in the eastern Mozambique Ocean around ~900 Ma with Azania and Tarim close to the eastern African margin (Fig. 3b). The suprasubduction system, constituted by Tarim–Azania–Afif–Abas–Lhasa (TAL) terranes/blocks, is characterized by volcanic arcs, intrusive rocks and terrane accretion (ca. 830–650 Ma) including migmatization and high-grade metamorphism (Fig. 2). Therefore, we suggest that the TAL terranes constitute the northern margin of the West Mozambique Ocean, and the Saharan, Congo-Tanzania cratons formed the southern margin of the West Mozambique Ocean (Fig. 4a, b).

Peak metamorphism, migmatization, and associated syn-collisional and syn-metamorphic orogenic granites within the TAL developed between 660 and 620 Ma. In our model, TAL collides with the eastern margin of the Congo craton and Saharan metacraton between 660–620 Ma with a general north–south progression. This orogenic belt extends from the ANS, Northern Tarim, Lhasa into Madagascar and the MB (Figs. 2 and 4c). The West Mozambique ocean is closed by continent–continent collision causing granulite-facies metamorphism in Lhasa, southern Madagascar, and the MB (Fig. 2). The metamorphic grade generally decreases from south to north, with lower-grade metamorphism in ANS and Tarim.

Between 590 and 520 Ma, high-grade metamorphism in southern India, Sri Lanka, Madagascar, and Mozambique was interpreted to represent the final collision between India with Azania during the Kuunga or Malagasy Orogeny and closure of the East Mozambique Ocean[2,3]. Continued compression and shortening between India with Azania and amalgamated Africa might induce the northward-directed escape of Tarim and Lhasa from the EAO via lateral escape tectonics[1,100,101].

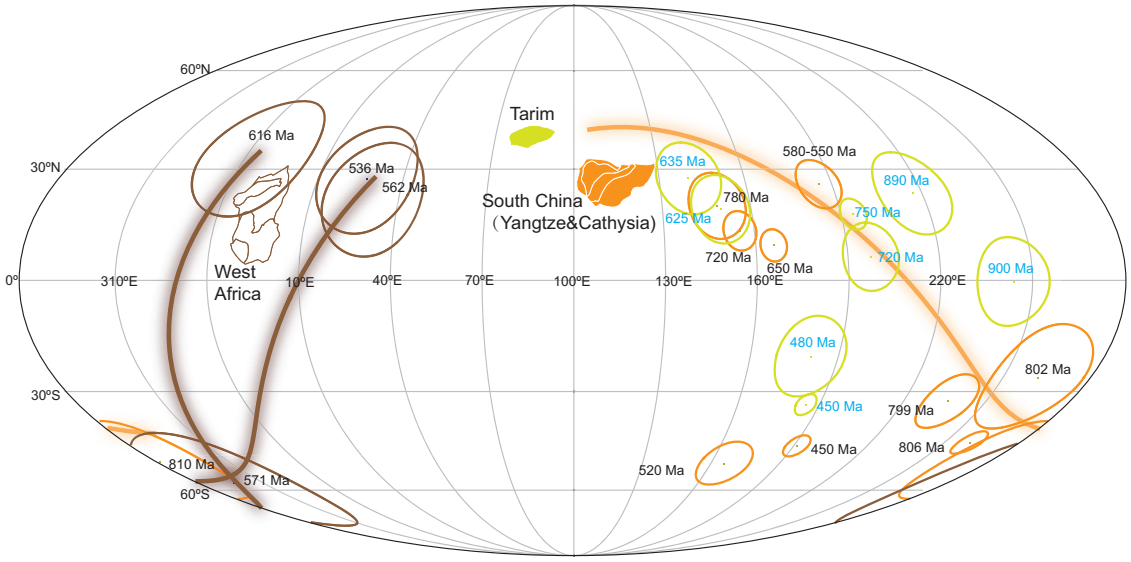

Fig. 5 Neoproterozoic–Early Paleozoic palaeomagnetic poles of South China (yellow) and Tarim (lime), and the Ediacaran poles from West Africa (brown). Orange and brown curves are fixed true polar wander trajectories (great circles) between 810–790 Ma for South China (orange) and 615–570 Ma for West Africa (brown). The TPW great circles are used to position the loci of subduction and to establish the relative paleo-longitude for South China, Tarim, and West Africa. All poles are listed in Supplementary Table 1.

Evolution of the Mozambique Ocean and growth of mega continent Gondwana. Geological records from the Neoproterozoic ANS suggest a marked change in the orientation of subduction zones in the Mozambique Ocean at ca. 720 Ma, from N–S to E–W directed[6]. Hence, we divide the evolution of the West Mozambique Ocean into two phases: spreading and closure before and after 720 Ma. Based on our interpretation of the paleomagnetic data from Tarim[89,90], we posit that Tarim and Lhasa separated from Rodinia before 850 Ma and the TAL blocks moved toward the equator opening the West Mozambique Ocean (Fig. 4a). The East Mozambique ocean developed as India-South China broke away from Rodinia at ca. 790 Ma[102]. The lengthy N–S striking subduction system in the East Mozambique ocean appears to be a relic of the circum-subduction system established during the tenure of Rodinia. Following breakup around 720 Ma, the Tonian to Cryogenian magmatic arcs and associated metamorphic basement of the TAL moved equatorward establishing a new E–W striking subduction girdle along the equator (Fig. 4b).

Breakup of Rodinia along the (present-day) western and Arctic margins of Laurentia (~720 Ma) established a new downwelling locus along the relic circum-subduction girdle (Fig. 4b). Subsequent motion of the continents was directed towards this new downwelling (Fig. 4c). The closure of the West Mozambique Ocean was related to subduction reorganization around 720 Ma from a predominately N–S strike to an E–W strike along with spreading in the East Mozambique Ocean[6]. The growth of the East Mozambique Ocean resulted from the southerly motion of the TAL blocks. Paleomagnetic data from South China indicate little latitudinal motion during the 780–635 Ma interval (Fig. 5), which would also apply to India if the two blocks remained in contact[102]. Final closure of the East Mozambique Ocean results from the post-635 Ma southward movement of South China–India (Fig. 4b, c).

Our reconstructions also differ from recent full-plate models[7] in that we use TPW to constrain the relative paleolongitude of the isolated blocks. Figure 5 illustrates the paleomagnetic data from South China and West Africa between 810–790 and 615–570 Ma with proposed TPW great-circle trajectories (brown and orange lines). Both South China and West Africa APWPs are close to, or overlap, the true polar wander paths. Our interpretation is that South China and West Africa were located near the downwelling girdle that surrounded the Rodinia supercontinent between 810–790 and 615–570 Ma, respectively[19]. In our reconstruction, the older (>750 Ma) subduction zone in the Mozambique Ocean is a relic subduction system related to the formation of the Rodinia. Therefore, they are subparallel with the true polar wander path (Fig. 4a). After 750–720 Ma, this relic subduction system ceased, and a new subduction system developed, which eventually led to the closure of Mozambique Ocean (Fig. 4b, c). The evolution of these subduction systems is consistent with the orthoversion supercontinent model[19, 103] because they lie along a girdle that is ~90° away from the center of Rodinia.

The "introversion" and "extroversion" models of supercontinent evolution predict that succeeding supercontinents will form either by closure of an interior ocean (such as the classic "Wilson-cycle" for the Atlantic Ocean)[18] or by the closure of an exterior ocean (such as the Pacific Ocean)[104]. In the general case, neither the introversion nor extroversion models provide an adequate explanation for the closure of young oceans (e.g. Rheic, Iapetus, and Tethys oceans during Gondwana and Pangea formations). In this specific case, the Mozambique Ocean is analogous to the younger oceans cited above. Its closure fate was sealed, as it just overlapped with the subduction girdle as suggested by the "orthorversion" model (Fig. 4b, c). The new tectonic reconstruction could be turned into a full plate reconstruction and used as a boundary condition of mantle flow models in future work.

Conclusions

Available Neoproterozoic geological and paleomagnetic data are compatible with Tarim in the southern hemisphere during the 900–650 Ma interval (Figs. 2 and 3). The Tarim, Lhasa, Arabia, Azania, and Afif–Abas terranes constitute an enlarged EAO along the northern margin of the West Mozambique Ocean. The West Mozambique Ocean grew in size until ~720 Ma. A post-720 Ma subduction reorganization developed almost orthogonal to the centroid of the former Rodinia supercontinent and resulted in the closure of the relatively young West Mozambique Ocean. This geometry is consistent with the orthoversion model of supercontinent evolution from Rodinia to Gondwana.

Methods

The metamorphic and magmatic rocks produced during mountain building is crucial to constrain geodynamic processes. We compiled zircon U-Pb ages between 1.1 and 0.52 Ga from Neoproterozoic metamorphic and magmatic rocks from Tarim, the Arabian–Nubian Shield, Oman, Mozambique belt, NW India, Madagascar, and the Lhasa terrane. The vast majority of ages in this compilation are from felsic to mafic intrusive or extrusive rocks, or their metamorphic equivalents. The dataset is available in Supplementary Data.

This manuscript is based on a tectonic reconstruction of the last billion years that was developed on the open-access software GPlates (www.gplates.org). The continent's shape and rotation files are from Merdith et al.[7] with the exception of the rotation parameters of the Tarim, Yangtze, Cathysia, India, Lhasa, and Congo-São Francisco, and Afif-Abas regions. These parameters are listed in Supplementary Table 2. The position of Tarim is constrained by using the palaeomagnetic data to place it in the southern hemisphere prior to 635 Ma.

Data availability

All data used in this manuscript are included in the published article (and its supplementary information files). In addition, all Supplementary geochronologic data have been uploaded to Figshare at https://doi.org/10.6084/m9.figshare.22873493

Received: 27 November 2022; Accepted: 8 June 2023;
Published online: 15 June 2023

References

1. Stern, R. J. Arc assembly and continental collision in the Neoproterozoic East Africa Orogen: implications of the consolidation of Gondwanaland. *Annu. Rev. Earth Planet. Sci.* **22**, 319–351 (1994).
2. Meert, J. G. A synopsis of events related to the assembly of eastern Gondwana. *Tectonophysics* **362**, 1–40 (2003).
3. Collins, A. S. & Pisarevsky, S. A. Amalgamating eastern Gondwana: the evolution of the circum-Indian orogens. *Earth-Sci. Rev.* **71**, 229–270 (2005).
4. Gray, D. R. et al. A Damara perspective on the assembly of southwestern Gondwana. *Geol. Soc. Lond. Spec. Publ.* **294**, 257–278 (2008).
5. Meert, J. G. & Lieberman, B. S. The Neoproterozoic assembly of Gondwana and its relationship to the Ediacaran–Cambrian transition. *Gondwana Res.* **14**, 5–21 (2008).
6. Collins, A. S. et al. Closure of the Proterozoic Mozambique Ocean was instigated by a late Tonian plate reorganization event. *Commun. Earth Environ.* **2**, 75 (2021).
7. Merdith, A. S. et al. Extending full-plate tectonic models into deep time: linking the Neoproterozoic and the Phanerozoic. *Earth-Sci. Rev.* **214**, 103477 (2021).
8. Merdith, A. S., Williams, S. E., Müller, R. D. & Collins, A. S. Kinematic constraints on the Rodinia to Gondwana transition. *Precambrian Res.* **299**, 132–150 (2017).
9. Seng¨or, A. M. C., Lom, N., Zabci, C., Sunal, G. & Oner, T. Reconstructing orogens without biostratigraphy: the Saharides and continental growth during the final assembly of Gondwana-Land. *Proc. Natl Acad. Sci. USA* **117**, 32278–32284 (2020).
10. Dalziel, I. W. D. Neoproterozoic–Paleozoic geography and tectonics: review, hypothesis, environmental speculation. *Geol. Soc. Am. Bull.* **109**, 16–42 (1997).
11. Squire, R., Campbell, I., Allen, C. & Wilson, C. Did the Transgondwanan Supermountain trigger the explosive radiation of animals on Earth? *Earth Planet. Sci. Lett.* **250**, 116–133 (2006).
12. Campbell, I. H. & Allen, C. M. Formation of supercontinents linked to increases in atmospheric oxygen. *Nat. Geosci.* **1**, 554–558 (2008).
13. Nimmo, F. Thermal and compositional evolution of the core. In *Treatise on Geophysics* (ed. Schubert, G.) 201–219 (Elsevier, 2015).
14. Meert, J. G., Levashova, N. M., Bazenhov, M. L. & Landing, E. Rapid changes of magnetic field polarity in the Late Ediacaran: linking the Cambrian evolutionary radiation and increased UV-B radiation. *Gondwana Res.* **34**, 149–157 (2016).
15. Lloyd, S. J., Biggin, A. J., Halls, H. C. & Hill, M. J. First paleointensity data from the Cryogenian and their potential implications for inner core nucleation. *Geophys. J. Int.* **226**, 66–77 (2021).
16. Yao, J. L. et al. Mariana type ophiolites constrain establishment of modern plate tectonic regime during Gondwana assembly. *Nat. Commun.* **12**, 4189 (2021).
17. Halverson, G. P., Hurtgen, M., Porter, S. M. & Collins, A. S. in *Events at the Precambrian-Cambrian Boundary: A Focus on Southwestern Gondwana* (eds Gaucher, C., Sial, A., Halverson, G. P. & Frimmel, H.) (Elsevier, 2010).
18. Murphy, J. B. & Nance, R. D. Do supercontinents introvert or extrovert: Sm–Nd isotope evidence. *Geology* **31**, 873–876 (2003).
19. Mitchell, R. N., Kilian, T. M. & Evans, D. A. D. Supercontinent cycles and the calculation of absolute palaeolongitude in deep time. *Nature* **482**, 208–211 (2012).
20. Li, Z. X. et al. Decoding Earth's rhythms: modulation of supercontinent cycles by longer superocean episodes. *Precambr. Res.* **323**, 1–5 (2019).
21. Flament, N., Bodur, F., Williams, S. E. & Merdith, A. E. Assembly of the basal mantle structure beneath Africa. *Nature* **603**, 846–851 (2022).
22. Rino, S. et al. The Grenvillian and Pan-African orogens: world's largest orogenies through geologic time, and their implications on the origin of superplume. *Gondwana Res.* **14**, 51–72 (2008).
23. Cawood, P. A., Martin, E. L., Murphy, J. B. & Pisarevsky, S. A. Gondwana's interlinked peripheral orogens. *Earth Planet. Sci. Lett.* **568**, 1–9 (2021).
24. Ge, R. et al. Neoproterozoic to Paleozoic long-lived accretionary orogeny in the northern Tarim Craton. *Tectonics* **33**, 302–329 (2014).
25. Zhang, Z. M. et al. The making of Gondwana: discovery of 650 Ma HP granulites from the North Lhasa, Tibet. *Precambr. Res.* **212–213**, 107–116 (2012).
26. Dalziel, I. W. D. Pacific margins of Laurentia and east Antarctica–Australia as a conjugate rift pair: evidence and implications for an Eocambrian supercontinent. *Geology* **19**, 598–601 (1991).
27. Fitzsimons, I. C. W. & Hulscher, B. Out of Africa: detrital zircon provenance of central Madagascar and Neoproterozoic terrane transfer across the Mozambique Ocean. *Terra Nova* **17**, 224–235 (2005).
28. Collins, A. & Windley, B. The tectonic evolution of central and northern Madagascar and its place in the final assembly of Gondwana. *J. Geol.* **110**, 325–339 (2002).
29. Johnson, P. R. The Arabian–Nubian Shield, an introduction: historic overview, concepts, interpretations, and future issues. In *The Geology of the Arabian-Nubian Shield* (eds Hamimi, Z. et al.) 1–38 (Springer, 2021).
30. Armistead, S. A. et al. Proterozoic basin evolution and tectonic geography of Madagascar during the Nuna/Columbia Supercontinent. *Tectonics* **40**, e2020TC006498, https://doi.org/10.1029/2020TC006498 (2021).
31. Mole, D. R., Barnes, S. J., Taylor, R. J. M., Kinny, P. D. & Fritz, H. A relic of the Mozambique Ocean in south-east Tanzania. *Precambr. Res.* **305**, 386–426 (2018).
32. Fritz, H. et al. Orogen styles in the East Africa Orogens: a review of the Neoproterozoic to Cambrian tectonic evolution. *J. Afr. Earth Sci.* **86**, 65–106 (2013).
33. Be'eri-Shlevin, Y. et al. The Sa'al volcano-sedimentary complex (Sinai, Egypt), a latest Mesoproterozoic volcanic arc in the northern Arabian Nubian Shield. *Geology* **40**, 403–406 (2012).
34. Eyal, M., Be'eri-Shlevin, Y., Eyal, Y., Whitehouse, M. J. & Litvinovsky, B. Three successive Proterozoic Island arcs in the Northern Arabian–Nubian Shield: evidence from SIMS U–Pb dating of zircon. *Gondwana Res.* **25**, 338–357 (2014).
35. Blades, M. L. et al. Age and Hafnium Isotope Evolution of Sudanese Butana and Chad Illuminates the Stenian to Ediacaran Evolution of the Southeast Sahara Metacraton. *Precambr. Res.* **362**, 106323 (2021).
36. Elisha, B., Katzir, Y. & Kylander-Clark, A. Ediacaran (620 Ma) high-grade regional metamorphism in the northern Arabian Nubian Shield: U–Th–Pb monazite ages of the Elat schist. *Precambr. Res.* **295**, 172–186 (2017).
37. Ali, K. A. et al. Age constraints on the formation and emplacement of Neoproterozoic ophiolites along the Allaqi-Heiani Suture, South Eastern Desert of Egypt. *Gondwana Res.* **18**, 583–595 (2010).
38. Gamal El Dien, H. et al. Neoproterozoic serpentinites from the Eastern Desert of Egypt: insights into Neoproterozoic mantle geodynamics and processes beneath the Arabian-Nubian Shield. *Precambr. Res.* **286**, 213–233 (2016).
39. Zoheir, B., Abd El-Rahman, Y., Kusky, T. & Xiong, F. New SIMS zircon U-Pb ages and oxygen isotope data for ophiolite nappes in the Eastern Desert of Egypt: implications for Gondwana assembly. *Gondwana Res.* **105**, 450–467 (2022).
40. Taylor, W. E. G., El-Kazzaz, Y. A. H. A., & Rashwan, A. A. An outline of the tectonic framework for the Pan-African orogeny in the vicinity of Wadi Um Relan area, south Eastern Desert, Egypt. In *Geoscientific Research in North-East Africa* (eds Schandelmeier, H. & Thorweihe, U.) 31–34 (CRC Press, 1993).
41. Bowden, S. et al. Evolution of the Western Ethiopian Shield revealed through U-Pb geochronology, petrogenesis, and geochemistry of syn-and post-tectonic intrusive rocks. *Precambr. Res.* **338**, 105588 (2020).
42. Johnson, P. R. et al. Late Cryogenian-Ediacaran history of the Arabian-Nubian Shield: a review of depositional, plutonic, structural, and tectonic events in the closing stages of the northern East African Orogen. *J. Afr. Earth Sci.* **61**, 167–232 (2011).
43. Robinson, F. A., Foden, J. D., Collins, A. S. & Payne, J. L. Arabian Shield magmatic cycles and their relationship with Gondwana assembly: insights from zircon U-Pb and Hf isotopes. *Earth Planet Sci. Lett.* **408**, 207–225 (2014).

44. Cox, G. M., Foden, J. & Collins, A. S. Late Neoproterozoic adakitic magmatism of the eastern Arabian Nubian Shield. *Geosci. Front.* **10**, 1981–1992 (2019).
45. Jarrar, G. H. et al. Geochemistry and P-T–t evolution of the Abu-Barqa Metamorphic Suite, SW Jordan, and implications for the tectonics of the northern Arabian-Nubian Shield. *Precambr. Res.* **239**, 56–78 (2013).
46. Bowring, S. A. et al. Geochronologic constraints on the chronostratigraphic framework of the Neoproterozoic Huqf Supergroup, Sultanate of Oman. *Am. J. Sci.* **307**, 1097–1145 (2007).
47. Mercolli, I. et al. Lithostratigraphy and geochronology of the Neoproterozoic crystalline basement of Salalah, Dhofar, sultanate of Oman. *Precambr. Res.* **145**, 182–206 (2006).
48. Rantakokko, N. E., Whitehouse, M. J., Pease, V. & Windley, B. F. Neoproterozoic evolution of the eastern Arabian basement based on a refined geochronology of the Marbat region, Sultanate of Oman. *Geol. Soc. Lond. Spec. Publ.* **392**, 107–127 (2004).
49. Blades, M. L. et al. Unravelling the Neoproterozoic accretionary history of Oman, using an array of isotopic systems in Zircon. *J. Geol. Soc.* **177**, 357–378 (2020).
50. Jacobs, J., Fanning, C. M., Henjes-Kunst, F., Olesch, M. & Paech, H.-J. Continuation of the Mozambique into East Antarctica: Grenville-age metamorphism and polyphase Pan-African high grade events in central Dronning Maud Land. *J. Geol.* **106**, 385–406 (1998).
51. Sommer, H., Kröner, A. & Lowry, L. Neoproterozoic eclogite- to high-pressure granulite-facies metamorphism in the Mozambique belt of east-central Tanzania: a petrological, geochemical and geochronological approach. *Lithos* **284–285**, 666–690 (2017).
52. Möller, A., Mezger, K. & Schenk, V. U-Pb dating of metamorphic minerals: Pan-African metamorphism and prolonged slow cooling of high pressure granulites in Tanzania, East Africa. *Precambr. Res.* **104**, 123–145 (2000).
53. Sommer, H., Kröner, A., Hauzenberger, C. H. & Muhongo, S. Reworking of Archaean and Palaeoproterozoic crust in the Mozambique belt of central Tanzania as documented by SHRIMP zircon geochronology. *J. Afr. Earth Sci.* **43**, 447–463 (2005).
54. Rossetti, F., Cozzupoli, D. & Phillips, D. Compressional reworking of the East African Orogen in the Uluguru Mountains of eastern Tanzania at c. 550 Ma: implications for the final assembly of Gondwana. *Terra Nova* **20**, 59–67 (2008).
55. Sommer, H. & Kröner, A. Ultra-high temperature granulite-facies metamorphic rocks from the Mozambique belt of SW Tanzania. *Lithos* **170–171**, 117–143 (2013).
56. Archibald, D. A. et al. Genesis of the Stenian-Tonian Dabolava Suite of west central Madagascar: implications for the evolution of the Mozambique Ocean and the formation of Rodinia. *J. Geol. Soc.* **175**, 111–129 (2017a).
57. Archibald, D. et al. Genesis of the Tonian Imorona-Itsindro Magmatic Suite in central Madagascar: insights from U-Pb, oxygen and hafnium isotopes in zircon. *Precambr. Res.* **281**, 312–337 (2016).
58. Archibald, D., Collins, A. S., Foden, J. D. & Razakamanana, T. Tonian Arc magmatism in Central Madagascar: the petrogenesis of the Imorona-Itsindro Suite. *J. Geol.* **125**, 271–297 (2017b).
59. Armistead, S. et al. Evolving marginal terranes during the Neoproterozoic supercontinent reorganisation: constraints from the Bemarivo Belt in northern Madagascar. *Tectonics* **38**, 2019–2035 (2019).
60. Moine, B., Boose, V., Paquette, J.-L. & Ortega, E. The occurrence of a Tonian-Cryogenian (~850 Ma) regional metamorphic event in central Madagascar and the geodynamic setting of the Imorona-Itsindro (~800 Ma) magmatic suite. *J. Afr. Earth Sci.* **94**, 58–73 (2014).
61. Zhou, J.-L. et al. New evidence for a continental rift tectonic setting of the Neoproterozoic Imorona-Itsindro Suite (central Madagascar). *Precambr. Res.* **306**, 94–111 (2018).
62. Thomas, R. J. et al. Geological evolution of the Neoproterozoic Bemarivo Belt, northern Madagascar. *Precambr. Res.* **172**, 278–300 (2019).
63. Jöns, N. & Schenk, V. Relics of the Mozambique Ocean in the central East African Orogen: evidence from the Vohibory Block of southern Madagascar. *J. Metamorph. Geol.* **26**, 17–28 (2008).
64. Boger, S. D. et al. The tectonic domains of southern and western Madagascar. *Precambr. Res.* **327**, 144–175 (2019).
65. Horton, F. et al. Focused radiogenic heating of middle crust caused ultrahigh temperatures in southern Madagascar. *Tectonics* **35**, 293–314 (2011).
66. Archibald, D. B. et al. Late syn- to post-collisional magmatism in Madagascar: the genesis of the Ambalavao and Maevarano Suites. *Geosci. Front.* **10**, 2063–2084 (2019).
67. Horton, F., Holder, R. M. & Swindle, C. R. An extensive record of orogenesis recorded in a Madagascar granulite. *J. Metamorph. Geol.* **40**, 287–305 (2022).
68. Tucker, R. D. et al. A new geological framework for southcentral Madagascar, and its relevance to the "out-of-Africa" hypothesis. *Precambr. Res.* **185**, 109–130 (2011).
69. Wang, C. et al. Recognition and tectonic implications of an extensive Neoproterozoic volcano-sedimentary rift basin along the southwestern margin of the Tarim Craton, northwestern China. *Precambr. Res.* **257**, 65–82 (2015a).
70. Zhang, C. L. et al. Neoproterozoicbimodal intrusive complex in the southwestern Tarim Block, Northwest China: age, geochemistry, and implications for the rifting ofRodinia. *Int. Geol. Rev.* **48**, 112–128 (2006).
71. Hu, P. et al. Early Neoproterozoic (ca. 900 Ma) rift sedimentation and mafic magmatism in the North Lhasa Terrane, Tibet: Paleogeographic and tectonic implications. *Lithos* **320–321**, 403–415 (2018).
72. Zeng, Y. C. et al. Petrogenesis and geodynamic signifiance of Neoproterozoic (~925 Ma) high-Fe-Ti gabbros of the Rentso ophiolite, Lhasa terrane, central Tibet. *Precambr. Res.* **314**, 160–169 (2018).
73. Dong, X., Zhang, Z. M., Niu, Y. L., Tian, Z. L. & Zhang, L. L. Reworked Precambrian metamorphic basement of the Lhasa terrane, southern Tibet: Zircon/Titanite U-Pb geochronology, Hf isotope and Geochemistry. *Precambr. Res.* **336**, 105496 (2020).
74. Liu, Y. M. et al. The passive margin of northern Gondwana during Early Paleozoic: evidence from the central Tibet Plateau. *Gondwana Res.* **78**, 126–140 (2020).
75. Meert, J. G., Pandit, M. K. & Kamenov, G. D. Further geochronologic and paleoamagnetic constraints on Malani (and pre-Malani) magmatism in NW India. *Tectonophysics* **608**, 1254 (2013). 1247.
76. Bhowmik, S. The current status of orogenesis in the central Indian tectonic zone: a view from its southern margin. *Geol. J.* **54**, 2912–2934 (2019).
77. Bhowmik, S. K., Dasgupta, S., Baruah, S. & Kalita, D. Thermal history of a Late Mesoproterozoic paired metamorphic belt (?) during Rodinia assembly: new insight from medium-pressure granulites from the Aravalli–Delhi Mobile Belt, Northwestern India. *Geosci. Front.* **9**, 335–354 (2018).
78. Singh, Y. K. et al. Tectonic setting of the Balaream–Kui–Surpagla–Kengora granulites of the South Delhi Terrane of the Aravalli Mobile Belt, NW India and its implication on correlation with the East African Orogen in the Gondwana assembly. *Precambr. Res.* **183**, 669–688 (2010).
79. Tiwari, S. K., & Biswal, T. K. Dynamics, EPMA Th-U-total Pb monazite geochronology and tectonic implications of deformational fabric in the lower-middle crustal rocks: a case study of Ambaji granulite, NW India. *Tectonics* **38**, 2232–2254 (2019).
80. De Wall, H. et al. Neoproterozoic geodynamics in NW India–evidence from Erinpura granites in the South Delhi Fold Belt. *Int. Geol. Rev.* **64**, 1051–1080 (2022).
81. Bhushan, S. K. Malani rhyolites—a review. *Gondwana Res.* **3**, 65–77 (2000).
82. Shakoor, M. A. et al. Early Neoproterozoic evolution of Southeast Pakistan: evidence from geochemistry, geochronology and isotopic composition of the Nagarparkar Igneous Complex. *Int. Geol. Rev.* **61**, 1398–1408 (2019).
83. De Wall, H. et al. Evolution and tectonic setting of the Malani–Nagarparkar Igneous Suite: a Neoproterozoic Silicic-dominated Large Igneous Province in NW India–SE Pakistan. *J. Asian Earth Sci.* **160**, 136–158 (2018).
84. Tucker, R. D., Ashwal, L. D. & Torsvik, T. H. U-Pb geochronology of Seychelles granitoids: a Neoproterozoic arc fragment. *Earth Planet. Sci. Lett.* **187**, 27–38 (2001).
85. Dharma Rao, C. V., Santosh, M. & Kim, S. W. Cryogenian volcanic arc in the NW Indian Shield: zircon SHRIMP U–Pb geochronology of felsic tuffs and implications for Gondwana assembly. *Gondwana Res.* **22**, 36–53 (2012).
86. Torsvik, T. H. et al. A Precambrian microcontinent in the Indian Ocean. *Nat. Geosci.* **6**, 223–227 (2013).
87. Zhao, J. H., Pandit, M. K., Wang, W. & Xia, X.-P. Neoproterozoic tectonothermal evolution of NW India: Evidence from geochemistry and geochronology of granitoids. *Lithos* **316–317**, 330–346 (2018).
88. Huang, B. C., Xu, B., Zhang, C. X., Li, Y. A. & Zhu, R. X. Palaeomagnetism of the Baiyi-sivolcanic rocks (ca. 740 Ma) of Tarim Northwest China: a continental fragment of Neoproterozoic Western Australia? *Precambr. Res.* **142**, 83–92 (2005).
89. Wen, B., Evans, D. A. D., Wang, C., Li, Y.-X. & Jing, X. A positive test for the Greater Tarim Block at the heart of Rodinia: mega-dextral suturing of supercontinent assembly. *Geology* **46**, 687–690 (2018).
90. Zhao, P., He, J., Deng, C., Chen, Y. & Mitchell, R. N. Early Neoproterozoic (870–820 Ma) amalgamation of the Tarim craton (northwestern China) and the final assembly of Rodinia. *Geology* **49**, 1277–1282 (2021).
91. Zhou, T., Ge, R., Zhu, W. & Wu, H. Is there a Grenvillian orogen in the southwestern Tarim Craton? *Precambr. Res.* **354**, 106053 (2021).
92. Wang, C., Zhang, J. H., Li, M., Li, R. S. & Peng, Y. Generation of ca. 900–870 Ma bimodal rifting volcanism along the southwestern margin of the Tarim Craton and its implications for the Tarim–North China connection in the Early Neoproterozoic. *J. Asian Earth Sci* **113**, 610–625 (2015b).
93. Meert, J. G. et al. The magnificent seven: a proposal for the modest revision of the quality index. *Tectonophysics* **790**, 228549 (2020).
94. Zhang, C. L. et al. A fragment of the ca. 890 Ma large igneous province (LIP) in southern Tarim, NW China: a missing link between S¯ao Francisco, Congo and North China cratons. *Precambr. Res.* **333**, 105428 (2019).

95. Eugênia Souza, M. et al. Time and isotopic constraints for Early Tonian basaltic magmatism in a large igneous province of the São Francisco–Congo paleocontinent (Macaúbas basin, Southeast Brazil). *Precambr. Res.* **373**, 106621 (2022).
96. Johnson, S. P. et al. Geochronology of the Zambezi Supracrustal Sequence, Southern Zambia: a record of Neoproterozoic divergent processes along the Southern Margin of the Congo Craton. *J. Geol.* **115**, 355–374 (2007).
97. Kouyaté, D. et al. U–Pb baddeleyite and zircon ages of 2040 Ma, 1650 Ma and 885 Ma on dolerites in the West African Craton (Anti-Atlas inliers): possible links to break-up of Precambrian supercontinents. *Lithos* **174**, 71–84 (2013).
98. Antonio, P. Y. J. et al. West Africa in Rodinia: high quality palaeomagnetic pole from the ~860 Ma Manso dyke swarm (Ghana). *Gondwana Res.* **94**, 28–43 (2021).
99. Verbaas, J. D. J. et al. A sedimentary overlap assemblage links Australia to northwestern Laurentia at 1.6 Ga. *Precambr. Res.* **305**, 19–39 (2018).
100. Jacobs, J. & Thomas, R. J. Himalayan-type indenter-escape tectonics model for the southern part of the late Neoproterozoic–early Paleozoic East African–Antarctic orogen. *Geology* **32**, 721–724 (2004).
101. Zhang, X. Z., Wang, Q., Dan, W., & Wyman, D. Locating Lhasa terrane in the Rodinia and Gondwana supercontinents: a key piece of the reconstruction puzzle. *Geol. Soc. Am. Bull.* https://doi.org/10.1130/B36152.1 (2022).
102. Jing, X. et al. Inverted South China: a novel configuration for Rodinia and its breakup. *Geology* **49**, 463–467 (2021).
103. Wang, C., Mitchell, R. N., Murphy, J. B., Peng, P. & Spencer, C. J. The role of mega continents in the supercontinent cycle. *Geology* **49**, 402–406 (2021).
104. Mitchell, R. N. et al. The supercontinent cycle. *Nat. Rev. Earth Environ.* **2**, 358–374 (2021).

Acknowledgements

We thank Drs. Alan Collins, Nicolas Flament, and one anonymous reviewer for their constructive comments. This work was supported by the National Natural Science Foundation of China (Grant Nos. 42272054, 42002208, and 42030307) and MOST Special Fund from the State Key Laboratory of Continental Dynamics.

Author contributions

C.W. designed the study, collected the data, and drafted the paper. X.-Q. J., clarified the relevant idea, design Figs. 3–5, and worked with C.W. on the writing of the paper. J.G.M. helped to write and to clarify the paper and helped to clarify some of the concepts. All authors contributed to the reviewing and editing of the manuscript.

Competing interests

The authors declare no competing interests.

Additional information

Supplementary information The online version contains supplementary material available at https://doi.org/10.1038/s43247-023-00883-6.

Correspondence and requests for materials should be addressed to Chao Wang or Xian-qing Jing.

Peer review information *Communications Earth & Environment* thanks Nicolas Flament, Alan Collins, and the other, anonymous, reviewer(s) for their contribution to the peer review of this work. Primary Handling Editors: João Duarte and Joe Aslin. A peer review file is available.